POLITECNICO DI TORINO Repository ISTITUZIONALE

Reduced carrier cooling and thermalization in semiconductor quantum wires

Original Reduced carrier cooling and thermalization in semiconductor quantum wires / Rota, L.; Rossi, Fausto; Goodnick, S. M.; Lugli, P.; Molinari, E.; Porod, W In: PHYSICAL REVIEW. B, CONDENSED MATTER ISSN 0163-1829 47:3(1993), pp. 1632-1635. [10.1103/PhysRevB.47.1632]
Availability: This version is available at: 11583/2498619 since:
Publisher: APS
Published DOI:10.1103/PhysRevB.47.1632
Terms of use:
This article is made available under terms and conditions as specified in the corresponding bibliographic description in the repository
Publisher copyright

(Article begins on next page)

Reduced carrier cooling and thermalization in semiconductor quantum wires

L. Rota and F. Rossi

Dipartimento di Fisica, Università di Modena, Via Campi 213/A, 41100 Modena, Italy

S. M. Goodnick

Department of Electrical and Computer Engineering, Oregon State University, Corvallis, Oregon 97331

P. Lugli

Dipartimento di Ingegneria Elettronica, II Università di Roma, Via E. Carnevale, 00173 Roma, Italy

E. Molinari*

Istituto "O. Corbino," Consiglio Nazionale delle Ricerche, Via Cassia 1216, 00189 Roma, Italy

W. Porod

Department of Electrical and Computer Engineering, University of Notre Dame, Notre Dame, Indiana 46556 (Received 5 June 1992)

By using a Monte Carlo analysis of the carrier relaxation in GaAs quantum wires following laser photoexcitation, we show that carrier cooling due to phonon emission and internal thermalization due to electron-electron interaction are significantly decreased with respect to bulk systems. This decreased thermalization is mainly attributed to the reduced efficiency of intersubband processes and to the reduced effect of electron-electron intrasubband scattering.

Most studies of transport in quantum-wire (QWR) and other mesoscopic systems have been primarily concerned with the near-equilibrium linear-response regime where quantum coherence effects are evident (see, for example, Ref. 1 and references therein). However, Cingolani and co-workers² have recently reported ultrafast pump and probe absorption studies of a quantum-wire system in which carrier relaxation was observed to be considerably slower than found in bulk systems under similar excitation conditions. Under such conditions, the carrier distribution is far from equilibrium, and many subbands of the quasi-one-dimensional (quasi-1D) wire system are occupied. The average energy of the carriers is well above that of the lattice, and phonon emission is dominant as carriers relax their energy in the return to equilibrium.

In such quasi-1D structures, the electron-phononscattering rate is substantially modified by quantization of the carrier motion due to the two-dimensional confining potential, as well as by changes in the Fröhlich-interaction Hamiltonian caused by phonon confinement and localization.³ Calculations of the electron-phonon-scattering rates in quasi-1D systems have been reported in the literature.³⁻⁶ Both intrasubband and intersubband scattering rates for bulklike polar optical phonons interacting with quantized electrons were reported, including self-energy corrections to account for broadening of the final density of states.3,6 More recently, scattering rates have been calculated for both quantized electrons and confined phonons in the 1D structure.⁴ Monte Carlo (MC) simulation of the carrier dynamics in quasi-1D systems under an applied electric field have been reported, and show features in the nonequilibrium distribution function arising from the reduced dimensionality of the system^{5,6} as well as real-space transfer out of the 1D system.7

The aim of the present Brief Report is to extend the analysis of nonequilibrium charge transport in quasi-1D systems by studying carrier relaxation following laser excitation. In particular, we consider the role of electronelectron scattering in the thermalization of the photoexcited carriers, an effect which has been neglected in previous treatments.⁵⁻⁷ Here the carrier dynamics is modeled using a k-space ensemble Monte Carlo simulation, 8 which allows a semiclassical transient analysis of the short-time evolution of the one-particle carrier distribution function during and after the generation of electron-hole pairs by the time-dependent optical pulse.

As a model system, we consider QWR structures such as those fabricated from multiple-quantum-well (MQW) samples by chemical etching.² This technique gives a GaAs rectangular quantum wire confined in the vertical growth direction (z) by $Al_xGa_{1-x}As$ layers, and free standing along the transverse direction (y). In the present MC simulation of this structure, electron-polar optical phonon (EP) scattering as well as the electron-electron (EE) interaction are included for both intrasubband and intersubband transitions. The EP and the EE interactions have been shown to dominate the subpicosecond transient regime in bulk GaAs (Refs. 9 and 10) and in GaAs/Al_xGa_{1-x}As MQW's (Refs. 11-13) for excitation energies below the threshold for intervalley transfer. We have deferred the study of scattering due to the photoexcited holes until later work to focus attention on the EE interaction alone.

Scattering due to the EE and EP interactions is treated using time-dependent perturbation theory within the ap-

47

proximation of Fermi's golden rule. To first order, the net scattering rate due to confined phonons in QW systems differs little from that calculated using bulk phonons, at least for well widths of about 100 Å or more. In the present work, we thus neglect phonon confinement effects due to the heterojunction interface and assume that the phonon modes are infinitely extended in the vertical z direction. Fuchs and Kliewer slab modes 14 are assumed in the lateral direction confined by air on either side. Broadening of the energy levels is also included to

account for inhomogeneities in the wire width as discussed elsewhere.^{3,4}

Carrier-carrier scattering in the QWR system is assumed to occur via a statically screened Coulomb interaction (the only affordable method in MC simulations), which is similar to that used in 3D (Ref. 8) and quasi-2D systems. The unscreened matrix element of the bare Coulomb potential between particle 1 of momentum k_1 in subband i with a second particle 2 of momentum k_2 initially in subband j is given by

$$H^{ee} = \frac{e^2}{2\pi\epsilon L} \int dz \int dy \int dz' \int dy' \varphi_i^1(y,z) \varphi_m^1(y,z) \varphi_j^2(y',z') \varphi_n^2(y',z')$$

$$\times \delta(k_1 + k_2 - k_1' - k_2') K_0 \left[|q_x| \sqrt{(y-y')^2 + (z-z')^2} \right],$$
(1)

where $\varphi_i(y,z)$ is the free-electron wave function in subband i, K_0 is the zeroth-order modified Bessel function, q_x is the wave vector exchanged in the x direction, k'_1-k_1 , and L is the simulated length of the wire. The final subbands after scattering are m for particle 1 and n for particle 2. The total scattering rate for an electron of wave vector k_1 in a given subband i is given by the sum over all final states for this electron and over all initial and final states of the partner electron. Neglecting for the moment degeneracy effects (degeneracy is accounted for later with a rejection technique), and using conservation of energy and momentum, the EE scattering rate becomes

$$\Gamma(k_1, E_{1i}) = \frac{e^4}{2\pi\epsilon^2 \hbar^3 L} \sum_{jmn} \left[\frac{|H^{\text{ee}}(q_1)|^2}{\left| \frac{q_1}{\mu'} + \left[\frac{k_1}{m'_1} - \frac{k_2}{m'_2} \right] \right|} + \frac{|H^{\text{ee}}(q_2)|^2}{\left| \frac{q_2}{\mu'} + \left[\frac{k_1}{m'_1} - \frac{k_2}{m'_2} \right] \right|} \right], \tag{2}$$

where μ' is the relative mass of the two carriers after scattering, and q_1 and q_2 are the two possible values for the exchanged momentum:

$$q_{x} = -\mu' \left[\frac{k_{1}}{m'_{1}} - \frac{k_{2}}{m'_{2}} \right] \pm \mu' \left[\frac{k_{1}^{2}}{m'_{1}^{2}} + \frac{k_{2}^{2}}{m'_{2}^{2}} - \frac{2k_{1}k_{2}}{m'_{1}m'_{2}} - \frac{k_{1}^{2}}{\mu'} \left[\frac{1}{m'_{1}} - \frac{1}{m_{1}} \right] - \frac{k_{2}}{\mu'} \left[\frac{1}{m'_{2}} - \frac{1}{m_{2}} \right] - \frac{2\Delta}{\mu' \tilde{n}^{2}} \right]^{1/2}, \quad (3)$$

where $\Delta = E'_1 + E'_2 - E_1 - E_2$ is the difference in the subband energy levels. As is evident from Eq. (3), for every pair of interacting electrons there are only two final states available. If, at the end of the scattering, the two carriers remain in their respective subbands, the only final state available is that in which the electrons exchange their crystal momentum. Such scattering is irrelevant if both particles originate from the same subband, since the two particles are indistinguishable. If the two electrons are in different subbands, this interaction produces a significant energy exchange between the subbands. We shall still refer to intrasubband scattering as the interaction of two electrons that lie in different subbands, as long as they remain in the same subbands after scattering. Intersubband scattering then refers to the case in which one or both of the electrons change subbands. The relative strength of intrasubband versus intersubband scattering depends on the magnitude of the EE form factor given by Eq. (1). Figure 1(a) shows a plot of this form factor as a function of q_x for several different types of intrasubband and intersubband transitions illustrated schematically in Fig. 1(b). The continuous line represents the intrasubband scattering between electrons in the first and the second subbands. The form factor peaks at small q_x , and is much larger than the intersubband form factors (shown

by the dashed and dotted lines, respectively) due to the orthogonality of the eigenfunctions. It is interesting to note that this type of scattering never creates new states in k space, and thus does not produce any thermalizing effect, only an energy redistribution between different subbands. The only scattering that enables a generation of new k states (and thus momentum relaxation) occurs for intersubband scattering. In this case, the difference of energy between the initial and final subbands enters into the conservation law and allows the creation of two completely new states. A typical transition is shown in Fig. 1(b) by the dashed line. As mentioned earlier, such intersubband scattering is greatly reduced due to the small form factor, and so thermalization due to carrier-carrier scattering is significantly reduced compared to that in higher-dimensional systems.

The screened scattering rate can be computed using the bare Coulomb potential dressed by the dielectric function of the carrier system:

$$H^{\mathrm{ee}}(q) {
ightarrow} rac{H^{\mathrm{ee}}(q)}{\left| arepsilon_{j,n}^{i,m}(q,\omega)
ight|} \; ,$$

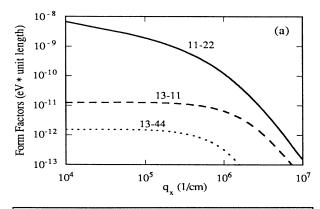
where ε is the dielectric matrix of the multisubband system. The static, long-wave limit is taken which allows

the analytic determination of the determinant above.

The MC method adopted here is substantially the same as that used in the simulation of bulk GaAs and GaAS/Al_xGa_{1-x}As QW's, with free motion in only the x direction. A rejection technique has been applied to take into account the Pauli exclusion principle in the final state after scattering, similar to that used in the 3D and 2D cases. As a model system, we have considered a 100-Å GaAs layer cladded by Al_{0.3}Ga_{0.7}As layers on either side in the z direction. The lateral width is chosen to be 300 Å, which gives a total of ten 1D subbands in the well.

In order to simplify the analysis, we have considered only photoexcitation from the heavy-hole band to the conduction band. The laser excitation is assumed to have a time duration of 50 fs and a spectral width of 20 meV. All the simulations were performed at a lattice temperature of 10 K with an equivalent density of 10^{17} cm⁻³. Electrons are generated in all the energetically accessible subbands (assuming that the $\Delta n = 0$ rule holds for transition between valence- and conduction-band subbands proportional to the final density of states).

In Fig. 2 we show the results of a simulation performed with a low excitation energy (43 meV) where only EE scattering is considered. The results are plotted versus the magnitude of k to illustrate the difference between the simulation results and those of a heated Maxwell-Boltzmann distribution (shown by the dotted line) of the same average energy as the injected distribution. In the QWR case [Fig. 2(a)], very little thermalization has oc-



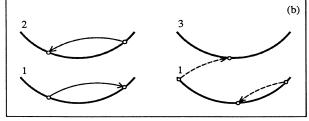


FIG. 1. (a) The form factor for EE transitions, Eq. (1), showing the intrasubband (solid line) contribution for two electrons lying in subbands 1 and 2, respectively, and the intersubband ones (dotted and dashed lines) for an electron jumping from subband 1 to 3 while the other remains in subband 1 (dashed line) or 4 (dotted line). (b) Schematic representations of the first two electronic transitions described above.

curred, even after 1 ps. In contrast to this result, the bulk case [Fig. 2(b)] is completely thermalized after 400 fs. The result illustrates the greatly reduced effect of intrasubband EE scattering in a 1D system in contrast to higher-dimensional systems due to the reduced phase space of the final state. Since thermalization in the presence of EE scattering alone may only proceed via intersubband events in a QWR system, the time scale is much longer than that required in 2D and 3D.

Figure 3 shows the combined effect of the EP and EE interactions, for both the QWR [Fig. 3(a)] and the bulk [Fig. 3(b)], respectively, when a higher excitation energy is used (170 meV). The peaks present in the QWR simulation correspond to the position of the subband minima indicated by the arrows shown in Fig. 3(a). The distribution function in the bulk is broadened with respect to the OWR case during the laser excitation, due to the strong effect of the EE interaction, and is completely thermalized after 300 fs. Again, the dotted lines in parts (a) and (b) correspond to a heated Maxwellian distribution at the temperature of the electron gas. In the QWR, the distribution function approaches that of heated Maxwellian only after 1 ps. The presence of both scattering mechanisms significantly increases the thermalization rate compared to that of EE scattering alone [Fig. 2(a)], since the emission of polar optical phonons allows the electrons to access new momentum states in conjunction with intrasubband EE scattering which redistributes energy among the various subbands. The combined thermalization rate, however, is still much slower than in an

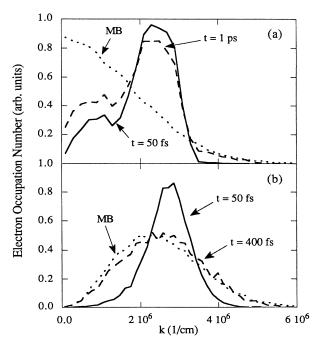


FIG. 2. (a) Electron occupation number in the QWR at two different times when only EE interaction is included as a function of k_x . The dotted line represents a heated Maxwellian at the temperature of the electron gas. (b) The same condition simulated in the bulk (in this case k is the modulus of the total momentum).

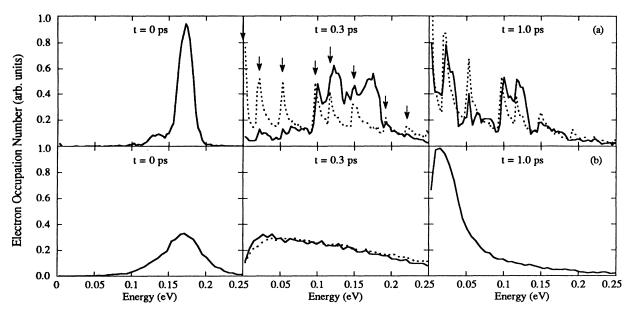


FIG. 3. (a) Electron occupation number in the QWR at three different times after the excitation including both EP and EE scattering. (b) The same conditions above repeated for the bulk.

equivalent bulk system, as illustrated by the comparison in Fig. 3. This slow thermalization in the QWR system is consistent with recent measurements² where a very slow thermalization was found.

In summary, we have presented a Monte Carlo study of photoexcited carrier relaxation in a quantum wire with realistic dimensions in which electron-electron and electron-polar optical phonon scattering is included. The energy relaxation rate due to electron-phonon scattering is reduced due to the relative strength of the intersub-

band versus intrasubband scattering. A strong reduction in the efficiency of the single-particle intercarrier interaction is shown, which results in a slow internal thermalization of the photoexcited electrons.

This work was partially supported by "Consorzio Nazionale di Fisica della Materia (INFM)," and by the EEC Commission under the Esprit Basic Science Project "NANOPT."

^{*}Present and permanent address: Dipartimento di Fisica, Università di Modena, via Campi 213/A, 41100 Modena, Italy.

¹Nanostructure Physics and Fabrication, edited by M. A. Reed and P. Kirk (Academic, Boston, 1989).

²R. Cingolani, H. Lage, L. Tapfer, H. Kalt, D. Heitmann, and K. Ploog, Phys. Rev. Lett. 67, 891 (1991).

³U. Bockelmann and G. Bastard, Phys. Rev. B 42, 8947 (1990).

⁴M. A. Stroscio, Phys. Rev. B **40**, 6428 (1989); K. W. Kim, M. A. Stroscio, A. Bhatt, R. Mickevicius, and V. V. Mitin, J. Appl. Phys. **70**, 319 (1991).

⁵S. Briggs and J. P. Leburton, Phys. Rev. B 38, 8163 (1988).

⁶D. Jovanovic, S. Briggs, and J. P. Leburton, Phys. Rev. B 42, 11 108 (1990).

⁷S. Briggs and J. P. Leburton, Phys. Rev. B **43**, 4785 (1991).

⁸C. Jacoboni and P. Lugli, The Monte Carlo Method for Semiconductor Device Simulation (Springer-Verlag, Wien, 1989).

⁹T. Elsaesser, J. Shah, L. Rota, and P. Lugli, Phys. Rev. Lett. 66, 1757 (1991).

¹⁰W. Z. Lin, W. Schoenlein, J. G. Fujimoto, and E. P. Ippen, IEEE J. Quantum Electron. QE-24, 267 (1988).

¹¹S. M. Goodnick and P. Lugli, Phys. Rev. B 37, 2578 (1988).

¹²S. M. Goodnick and P. Lugli, Phys. Rev. B 38, 10135 (1988).

¹³S. M. Goodnick and P. Lugli, in *Hot Carriers in Semiconductor Nanostructures: Physics and Applications*, edited by J. Shah (Academic, New York, 1992), pp. 191-234.

¹⁴R. Fuchs and K. L. Kliewer, Phys. Rev. **140**, A2076 (1965).